Smart Materials

DOI: 10.1002/anie.201101054

Polyelectrolyte Multilayer Films for Building Energetic Walking Devices**

*Ying Ma, Yuanyuan Zhang, Baisheng Wu, Weipeng Sun, Zhengguang Li, and Junqi Sun**

Dedicated to Professor Jiacong Shen on the occasion of his 80th birthday.

Artificial smart materials capable of reversible and controlled two- or three-dimensional shape changes in response to external stimuli are of key importance in fabricating actuators, switches, cantilever sensors, artificial muscles, and even microrobotics.[1] Various smart materials, including gels,[2] shape-memory polymers,[3] and conjugated polymers,[4] have been developed that respond to external stimuli such as temperature,[5] humidity,[6] light,[1b,d,7] electric fields,[1c] and solvent composition or pH.[8] For several applications, especially actuators in microrobotics, "energetic" materials that produce a fast response and convert chemical or physical energy to mechanical motion in a highly efficient way are urgently required, but their fabrication is challenging.[1e,9]

Layer-by-layer (LbL) assembled polyelectrolyte multilayer (PEM) films of alternating polyanions and polycations have long been recognized as a wide variety of important soft materials.[10] Polyelectrolyte multilayer films with diverse compositions and mechanical flexibility, which provide durability against repeated deformation,[11] can be designed to respond to different stimuli.[10b,12] However, their functionality as actuators is largely unexplored, as they are usually deposited on undeformable substrates. Herein we report fabrication of a powerful actuator by attaching a flexible non-water-adsorbing layer of UV-cured Norland Optical Adhesive 63 (NOA 63) on top of a PEM film of thermally cross-linked poly(acrylic acid) (PAA)/poly(allylamine hydrochloride) (PAH), and releasing the bilayer film from the PEM substrate. This bilayer actuator could drive a walking device carrying a load 120 times heavier than the actuator to walk steadily on a ratchet substrate under periodic alternation of the relative humidity (RH) between 11 and 40%. The unprecedented load-carrying capacity and fast response of the walking device suggest that PEM films will be promising for various energetic actuators and actuator-based devices.

The bilayer film consists of a layer of thermally cross-linked 30-bilayer PAA/PAH film [denoted (PAA/PAH)*30] fabricated by LbL assembly,[13] which is subsequently spin-coated with a layer of UV-cured NOA 63, which is a mercapto ester-type UV-curable prepolymer. Free-standing (PAA/PAH)*30/NOA 63 bilayer films with large areas can be released from substrates by immersing films deposited on poly(diallyldimethylammonium chloride) (PDDA)-modified silicon wafers in an aqueous solution with a pH of 2.0.[13] The cross-sectional SEM image in Figure 1b shows that the PAA/PAH and NOA 63 layers have constant thicknesses of 1.79 ± 0.01 μm and 10.37 ± 0.06 μm, respectively. The NOA 63 layer is in intimate contact with the underlying PAA/PAH layer. The free-standing (PAA/PAH)*30/NOA 63 bilayer films are

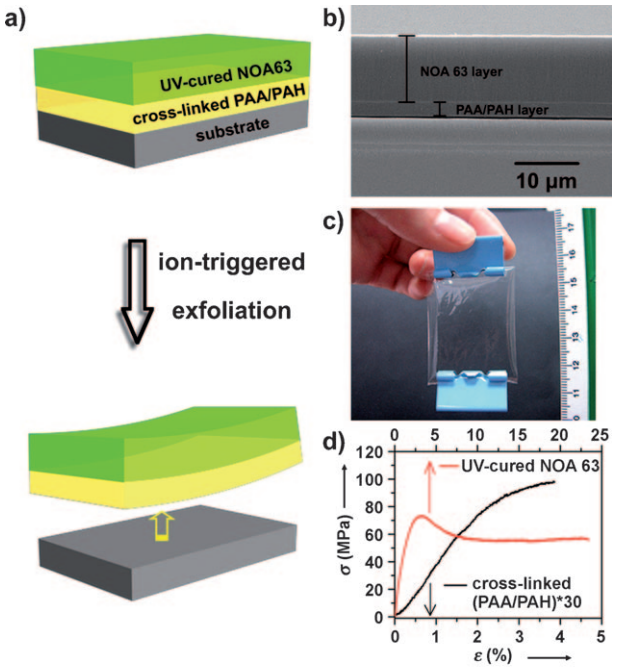

Figure 1. a) Schematic illustration of the (PAA/PAH)*30/NOA 63 bilayer film, and the process of releasing it from the substrate. b) Cross-sectional SEM image of the (PAA/PAH)*30/NOA 63 free-standing film transferred onto a silicon wafer. c) Photograph of the (PAA/PAH)*30/NOA 63 free-standing film with a size of 3.0×4.0 cm. The clip hung at the bottom of the film has a mass of 4.0 g. d) Typical stress–strain curves for thermally cross-linked (PAA/PAH)*30 and UV-cured NOA 63 layers.

[*] Dr. Y. Ma, Y. Zhang, Prof. J. Sun
State Key Laboratory of Supramolecular Structure and Materials
College of Chemistry, Jilin University
Chanchun 130012 (P. R. China)
Fax: (+86) 431-85193-421
E-mail: sun_junqi@jlu.edu.cn
Prof. B. Wu, Dr. W. Sun, Dr. Z. Li
Department of Mechanics and Engineering Science
School of Mathematics, Jilin University
Changchun 130012 (P. R. China)

[**] This work was supported by the National Natural Science Foundation of China (NSFC grant no. 20774035), the National Basic Research Program (2007CB808000, 2009CB939701) and Ministry of Education.

Supporting information for this article is available on the WWW under http://dx.doi.org/10.1002/anie.201101054.

transparent and mechanically robust (Figure 1c). The typical stress–strain curves of the thermally cross-linked PAA/PAH and UV-cured NOA 63 layers (Figure 1d) indicate that each individual layer is flexible but mechanically robust. The thermally cross-linked PAA/PAH layer has an ultimate tensile strength σ_u of 96 ± 3 MPa and Young's modulus E of 4.3 ± 0.1 GPa, while the σ_u and E values of the NOA 63 layer are 81 ± 7 MPa and 4.0 ± 0.5 GPa, respectively. The ultimate strain ε of the NOA 63 layer (22 ± 4%) is clearly higher than that of the cross-linked PAA/PAH film (3.3 ± 0.5%). The mechanical properties of PEM films have been thoroughly studied.[14]

The cross-linked PAA/PAH layer has great ability to adsorb/desorb water with increasing/decreasing environmental humidity, which results in swelling/shrinking of the PAA/PAH films.[13b] The cross-linked PAA/PAH layer, which has a linear coefficient of moisture expansion of $(6.0 \pm 1.1) \times 10^{-4}$/% RH (Supporting Information, Figure S1), adsorbs water to 12.5% of its original mass when the RH increases from 0 to 100%. By contrast, the NOA 63 layer is inert to humidity change. The widely differing water-responsive properties of the PAA/PAH and NOA 63 layers, combined with their high flexibility and mechanical robustness, suggest that the (PAA/PAH)*30/NOA 63 bilayer films would be excellent humidity-responsive actuators. A free-standing (PAA/PAH)*30/NOA 63 film (0.5×0.8 cm), fixed at one edge on a filter paper, was nearly flat at room temperature (25°C) and 12% RH (Figure 2a). When the RH was decreased from 12 to 5% by a gentle flow of dry nitrogen over the film, the upper PAA/PAH layer contracted as it lost adsorbed water and the underlying NOA 63 layer remained unchanged. This large mismatch in contraction led to interfacial stress between the PAA/PAH and NOA 63 layers, which bent the bilayer film clockwise to nearly 180° within 9 s. When the RH was increased to its original level (12%), the bilayer film returned to its initial shape within 27 s because of extension of the PAA/PAH layer on water adsorption. The bilayer actuator shows repeated and reproducible bending/unbending responses to humidity alternation, without any fatigue over time (Figure 2b).

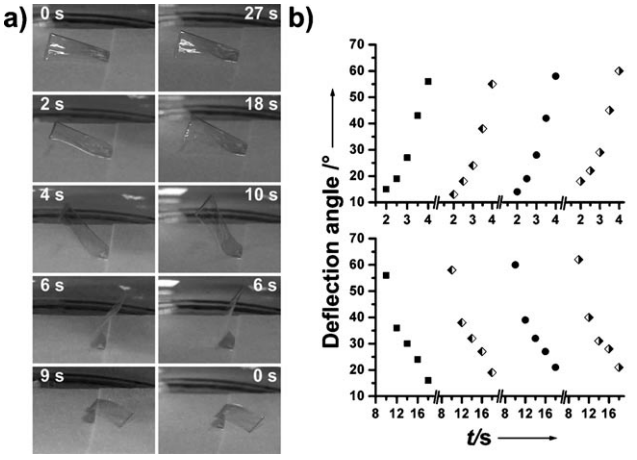

Figure 2. a) Time profiles of bending and unbending movements of a (PAA/PAH)*30/NOA 63 actuator (0.5×0.8 cm) with changing humidity. The humidity in the left column changed from 12 to 5% RH, and that in the right column from 5 to 12% RH. b) Time-dependent bending angles of a (PAA/PAH)*30/NOA 63 actuator when the humidity is changed from 12 to 5% RH (top) and from 5 to 12% RH (bottom). The bilayer (PAA/PAH)*30/NOA 63 film always takes 4 s to bend to a deflection angle of approximately 57° and 8 s to unbend from this deflection angle to its original shape.

The excellent humidity-responsive bending/unbending of the (PAA/PAH)*30/NOA 63 actuators was further explored to build walking devices. Two pieces of polyethylene terephthalate (PET) plate were connected as claws at opposite ends of the actuator (Figure 3a). The actuator drove unidirectional

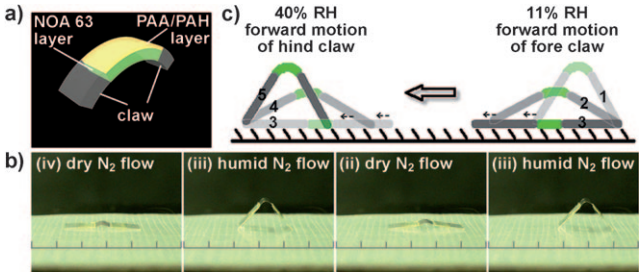

Figure 3. a) Configuration of the walking device, composed of the (PAA/PAH)*30/NOA 63 actuator and two claws. The top layer is thermally cross-linked PAA/PAH film, and the bottom layer UV-cured NOA 63. b) Locomotion of the walking device on a polyethylene (PE) ratchet substrate when RH is alternated between 11 and 40%. The actuator is 4.3 mm wide and 2.0 mm long. The claws are the same width as the actuator and 4.0 mm long. The walking device moves from right to left. c) Breakdown drawings of walking movements of the device on the ratchet substrate driven by changing humidity.

walking of the device on a ratchet substrate when RH alternated between 40 and 11% (Figure 3b and Supporting Information, Movie 1). Figure 3c depicts walking of the device on a ratchet substrate. Initially, the whole device bent upward into an arch, because the upper PAA/PAH layer was swollen at an RH of 40%. The PAA/PAH layer then contracted with decreasing humidity (11% RH), which made the walking device stretch forward along the direction of the indentation array (1→2→3). During stretching, the fore claw moved forward while the hind claw was fixed by one of the indentations on the substrate. Then, when RH was increased to 40%, the PAA/PAH layer became swollen again and the device bent into an arch (3→4→5), which led to movement of the hind claw toward the fore claw, as the fore claw was fixed by the indentation. With alternation of the environmental humidity, the device walked unidirectionally in a step-by-step way, driven by the interfacial stress between the PAA/PAH and NOA 63 layers. The orientation of the indentations in the ratchet substrate sets the movement of the walking device along a predetermined but controllable path.

The (PAA/PAH)*30/NOA 63 actuator has many attributes that would be required for construction of walking devices for cargo transportation. It is lightweight at only 0.3 mg for a 4.3×2.0 mm actuator. The two claws have a mass of 7.1 mg. Therefore, the (PAA/PAH)*30/NOA 63 actuator can drive steady and rapid movement of a device that is 24 times the actuator's mass. Surprisingly, the walking device

could walk even when more pairs of PET plates were attached to the claws, which increased the load. The step length of the walking device, which is the distance between the fully bent and unbent positions of the hind claw in the device, decreases with increasing load. As indicated in Figure 4, the step lengths

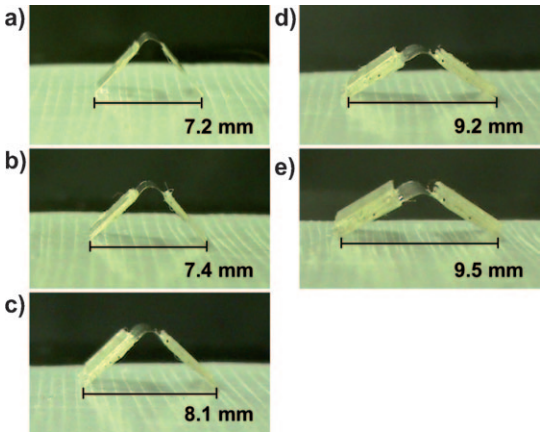

Figure 4. Photographs of walking devices with different loads on the ratchet substrate when bent to an arch at 40% RH. The loads are 24 (a), 48 (b), 72 (c), 96 (d), and 120 (e) times the actuator mass. The walking devices have a total length of 10 mm.

of the device with loads of 24, 48, 72, 96, and 120 times the actuator mass are 2.8, 2.6, 1.9, 0.8, and 0.5 mm, respectively. The walking device with five pairs of PET claws, which had a total mass of 36.2 mg, walked in a clumsy and slow manner when the distance between adjacent indentations was 0.8–1.0 mm. With the same humidity changes, walking of this device became steady when the distance between the adjacent indentations was decreased to about 0.5 mm (Supporting Information, Movies 2 and 3). Therefore, the (PAA/PAH)*30/NOA 63 actuator can drive a device that is 120 times heavier than the actuator to walk under environmental humidity alternation between 11 and 40% RH.

Theoretical analysis of the walking device on a ratchet substrate was conducted on the basis of double-beam theory, to understand its exceedingly high load-carrying capacity (Supporting Information, Figures S2–S4).[15] For a walking device driven by a bilayer actuator with unit width, we analyzed the stress generated during the bending process which occurred on forward motion of the hind claw. The bending of the bilayer actuator in the walking device was induced by the humidity increase from m_0 to m_1 and the loads on the claws. Therefore, the curvature of the bilayer actuator in the walking device with a load $1/\rho_b$ is the sum of the curvature of the load-free bilayer actuator induced by the change in environment humidity ($1/\rho_h$) and the curvature of the actuator resulting from the load on the claw ($1/\rho_m$), which gives Equation (1)

$$\frac{1}{\rho_b} = \frac{6k_1k_2(1+k_2)(m_1-m_0)(\varepsilon_1-\varepsilon_2)}{h_2[1+k_1k_2(4+6k_2+4k_2^2+k_1k_2^3]} - \frac{GL\cos\theta}{2(EI)_e} \quad (1)$$

where $k_1 = E_1/E_2$ and $k_2 = h_1/h_2$; E_1, h_1, and ε_1 are the Young's modulus, thickness, and linear coefficient of moisture expansion for the cross-linked PAA/PAH film, respectively; E_2, h_2, ε_2 are the corresponding values for the NOA 63 layer; L and l are the length of the claws and the bilayer actuator, respectively, and both these elements have the same width d; G is the load per unit width of one claw, including the mass of the claw itself; θ is the angle between the axis of the hind claw and the substrate surface; and $(EI)_e$ is the equivalent flexural rigidity of the bilayer actuator. In the walking device, the angle θ between the claw and the substrate changes from 0 to $\pi/2$. We predict that the maximum load could be determined by letting $\theta \rightarrow 0$, which gives Equation (2).

$$G_{max} = \frac{E_1h_1h_2(1+k_2)(m_1-m_0)(\varepsilon_1-\varepsilon_2)}{L(1+k_1k_2)} \quad (2)$$

where G_{max} denotes the maximum load of one claw in a strip of the actuator with unit width. The maximum load for the walking device with width d is thus given by Equation (3).

$$F_{max} = 2dG_{max} = \frac{2dE_1h_1h_2(1+k_2)(m_1-m_0)(\varepsilon_1-\varepsilon_2)}{L(1+k_1k_2)} \quad (3)$$

From Equation (3), we can derive that the maximum load of the device is as high as 0.375 mN, which is approximately 128 times heavier than the actuator, when the RH is alternated between 11 and 40% (Supporting Information, Table S1). The maximum load derived from Equation (3) agrees well with the experimental observation of a walking device with a load 120 times heavier than the actuator, which walked clumsily on the ratchet substrate with a distance of 0.8–1.0 mm between adjacent indentations. The theoretical analysis demonstrates that, besides the mechanically robust but flexible NOA 63 supporting layer, the exceedingly high load-carrying capacity of the walking device mainly originates from the good combination of high Young's modulus and large linear coefficient of moisture expansion of the PAA/PAH layer. Although film materials with high Young's modulus or large coefficient of expansion are easily available, a good combination of these two key attributes in one film is difficult to achieve. Thus, LbL assembly, which enables precise control of film composition and structure, is promising for fabricating such films for use as powerful actuators. Moreover, the thin LbL-assembled PAA/PAH layer facilitates rapid water adsorption/desorption, and therefore fast response of the walking device toward environmental humidity changes, because the diffusion time of the solvent is generally proportional to the square of the film thickness.[16]

In summary, we have demonstrated the fabrication of an energetic walking device driven by a powerful humidity-responsive bilayer actuator comprising an action layer of thermally cross-linked PAH/PAA films and a supporting layer of UV-cured NOA 63. Mechanical analysis indicates that a good combination of high Young's modulus, large linear coefficient of moisture expansion, and rapid water-adsorption/desorption ability of the cross-linked PAH/PAA films is of key importance for functioning as a powerful actuator in an energetic walking device. Given the diverse compositions of polyelectrolyte films and the wide selection of partner

supporting layers for bilayer actuators, we believe that the present work will open a new avenue for design of various actuators. These actuators can be used to build miniaturized devices capable of fast response to a wide variety of stimuli and efficient energy transfer.

Experimental Section

Materials: PAA ($M_w \approx 1800$), PAH ($M_w \approx 56000$), and PDDA (20 wt%, $M_w \approx 100000$–200000) were purchased from Sigma-Aldrich. NOA 63 was purchased from Norland Products Inc. NOA 63 can be cured when exposed to UV light in the range of 350–380 nm. All chemicals were used without further purification. The concentration of the dipping solutions for PAA/PAH multilayer fabrication was 1 mg mL^{-1} in 18 MΩ Millipore water, and pH was adjusted with 1M HCl or 1M NaOH.

Preparation of bilayer free-standing films and walking devices: Preparation of (PAA/PAH)*30/NOA 63 bilayer film involves LbL deposition of the PAA/PAH layer and spin-coating of the NOA 63 layer on top of the PAA/PAH layer. LbL deposition of the (PAA/PAH)*30 films was reported in our previous publications and is described in the Supporting Information.[13] The (PAA/PAH)*30 film was thermally cross-linked by heating at 180°C for 2 h in a vacuum oven. A 10 μm-thick layer of NOA 63 was spin-coated onto the cross-linked PAA/PAH layer at 4000 rpm for 2 min. The NOA 63 layer was cross-linked by irradiating the layer with a 250 W UV lamp ($\lambda =$ 365 nm) for 5 min at a distance of 12 cm from the source. A free-standing (PAA/PAH)*30/NOA 63 film was obtained by immersing the bilayer film deposited on the PDDA-modified silicon wafer into an aqueous solution with a pH of 2.0 for 30 min.[13] To facilitate release of the bilayer film, the edges of the film were cut off with a knife. The bilayer film was released by breaking the electrostatic interaction of the first PAA layer of the bilayer film with the underlying PDDA layer in a highly acidic aqueous solution.[13] The walking device was produced by attaching two PET plates as claws at opposite ends of the bilayer actuator.

Instruments and methods: The thickness and cross-sectional profile of the bilayer actuator were characterized with a XL30 ESEM FEG SEM. Stress–strain curves and the linear coefficient of moisture expansion of the thermally cross-linked PAA/PAH and UV-cured NOA 63 layers were measured with a mechanical strength microtest device (410R250, Test Resources, Shakopee, MN).

Received: February 11, 2011
Published online: May 20, 2011

Keywords: actuators · layer-by-layer assembly · materials science · smart materials · thin films

[1] a) M. A. Cohen Stuart, W. T. S. Huck, J. Genzer, M. Müller, C. Ober, M. Stamm, G. B. Sukhorukov, I. Szleifer, V. V. Tsukruk, M. Urban, F. Winnik, S. Zauscher, I. Luzinov, S. Minko, *Nat. Mater.* **2010**, *9*, 101–113; b) Y. Yu, T. Maeda, J. Mamiya, T. Ikeda, *Angew. Chem.* **2007**, *119*, 899–901; *Angew. Chem. Int. Ed.* **2007**, *46*, 881–883; c) T. Fukushima, K. Asaka, A. Kosaka, T. Aida, *Angew. Chem.* **2005**, *117*, 2462–2465; *Angew. Chem. Int. Ed.* **2005**, *44*, 2410–2413; d) M. Yamada, M. Kondo, R. Miyasato, Y. Naka, J. Mamiya, M. Kinoshita, A. Shishido, Y. Yu, C. J. Barrettc, T. Ikeda, *J. Mater. Chem.* **2009**, *19*, 60–62; e) A. W. Feinberg, A. Feigel, S. S. Shevkoplyas, S. Sheehy, G. M. Whitesides, K. K. Parker, *Science* **2007**, *317*, 1366–1370; f) M. Camacho-Lopez, H. Finkelmann, P. Palffy-Muhoray, M. Shelley, *Nat. Mater.* **2004**, *3*, 307–310; g) S. Maeda, Y. Hara, T. Sakai, R. Yoshida, S. Hashimoto, *Adv. Mater.* **2007**, *19*, 3480–3484.

[2] S. Ahn, R. M. Kasi, S.-C. Kim, N. Sharma, Y. X. Zhou, *Soft Matter* **2008**, *4*, 1151–1157.

[3] C. Liu, H. Qin, P. T. Mather, *J. Mater. Chem.* **2007**, *17*, 1543–1558.

[4] E. Smela, *Adv. Mater.* **2003**, *15*, 481–494.

[5] R. Yoshida, K. Uchida, Y. Kaneko, K. Sakai, A. Kikuchi, Y. Sakurai, T. Okano, *Nature* **1995**, *374*, 240–242.

[6] J. Kopeček, *Nature* **2002**, *417*, 388–391.

[7] S. Ahir, E. M. Terentjev, *Nat. Mater.* **2005**, *4*, 491–495.

[8] Z. Hu, X. Zhang, Y. Li, *Science* **1995**, *269*, 525–527.

[9] S. Kobatake, S. Takami, H. Muto, T. Ishikawa, M. Irie, *Nature* **2007**, *446*, 778–781.

[10] a) G. Decher, *Science* **1997**, *277*, 1232–1237; b) J.-A. Hiller, J. D. Mendelsohn, M. F. Rubner, *Nat. Mater.* **2002**, *1*, 59–63; c) A. B. South, L. A. Lyon, *Angew. Chem.* **2010**, *122*, 779–783; *Angew. Chem. Int. Ed.* **2010**, *49*, 767–771; d) C. Y. Jiang, S. Markutsya, Y. Pikus, V. V. Tsukruk, *Nat. Mater.* **2004**, *3*, 721–728; e) Y. Li, L. Li, J. Q. Sun, *Angew. Chem.* **2010**, *122*, 6265–6269; *Angew. Chem. Int. Ed.* **2010**, *49*, 6129–6133; f) X. Zhang, H. Chen, H. Zhang, *Chem. Commun.* **2007**, 1395–1405.

[11] J. L. Lutkenhaus, K. D. Hrabak, K. McEnnis, P. T. Hammond, *J. Am. Chem. Soc.* **2005**, *127*, 17228–17234.

[12] a) Y. Liu, M. Zhao, D. E. Bergbreiter, R. M. Crooks, *J. Am. Chem. Soc.* **1997**, *119*, 8720–8721; b) J. A. Jaber, J. B. Schlenoff, *Macromolecules* **2005**, *38*, 1300–1306.

[13] a) Y. Ma, J. Q. Sun, J. C. Shen, *Chem. Mater.* **2007**, *19*, 5058–5062; b) Y. Ma, J. Q. Sun, *Chem. Mater.* **2009**, *21*, 898–902.

[14] a) F. Dubreuil, N. Elsner, and A. Fery, *Eur. Phys. J. E* **2003**, *12*, 215–221; b) O. I. Vinogradova, O. V. Lebedeva, B.-S. Kim, *Annu. Rev. Mater. Res.* **2006**, *36*, 143–178.

[15] S. Timoshenko, *Theory of Elastic Stability*, McGraw-Hill, New York, **1961**.

[16] T. Tanaka, D. J. Fillmore, *J. Chem. Phys.* **1979**, *70*, 1214–1218.

